Chem Soc Rev

RSC Publishing

TUTORIAL REVIEW

View Article Online
View Journal | View Issue

Mechanochemical reactions and syntheses of oxides

Cite this: *Chem. Soc. Rev.*, 2013, **42**, 7507

Vladimir Šepelák,†*[ab] Andre Düvel,[bc] Martin Wilkening,[d] Klaus-Dieter Becker[be] and Paul Heitjans[bc]

Received 10th November 2012

DOI: 10.1039/c2cs35462d

www.rsc.org/csr

Technological and scientific challenges coupled with environmental considerations have prompted a search for simple and energy-efficient syntheses and processing routes of materials. This *tutorial review* provides an overview of recent research efforts in non-conventional reactions and syntheses of oxides induced by mechanical action. It starts with a brief account of the history of mechanochemistry. Ensuing discussions will review the progress in homogeneous and heterogeneous mechanochemical reactions in oxides of various structures. The review demonstrates that the event of mechanically induced reactions provides novel opportunities for the non-thermal manipulation of materials and for the tailoring of their properties.

Key learning points

1. What is mechanochemistry? Its historical milestones.
2. What kind of mechanochemical reactions can be induced in oxides?
3. What is the nature of mechanically induced disorder in oxides?
4. How can surface effects be separated from the bulk effects in mechanosynthesized oxide nanoparticles?
5. What is the range of thermal stability of oxides prepared by mechanochemical routes?

1. Mechanochemistry as a branch of chemistry

The energy needed for the activation of chemical reactions is usually provided by heat, light, or electrical potential. Correspondingly, terms such as *thermochemistry*, *photochemistry*, or *electrochemistry* are generally common in the chemistry literature. A fundamentally different way of initiating or accelerating a chemical reaction is the use of mechanical force (action). Mechanically induced chemistry (the so-called *mechanochemistry*) has a long history and continues to be of high importance. We refer the reader to ref. 1–3 for detailed accounts of the history of mechanochemistry. Nevertheless, some milestones of mechanochemistry should be mentioned here. According to some authors,[1–3] the latter began with Theophrastus of Eresos (371–287 B.C.), a student of Aristotle. In his book ''De Lapidibus'' (''On Stones''), he reported that native cinnabar, when rubbed in a brass mortar with a brass pestle in the presence of vinegar, yields metallic mercury. Establishing *mechanochemistry* as a separate branch of chemistry is usually attributed to Matthew Carey Lea (Fig. 1), who demonstrated at the end of the nineteenth century that certain compounds react differently under the influence of mechanical action and heat. He observed the decomposition of silver and mercuric halides by trituration in a porcelain mortar although the same compounds are known to melt or sublime undecomposed when heated.[4] These experiments are considered nowadays to be the first systematic investigations on the chemical effects of mechanical action.[1] Note that scientific contributions of Michael Faraday on the effect of mechanical energy on the reduction of AgCl with Zn, Sn, Fe, and Cu often remain forgotten.[5] In 1919, the term *mechanochemistry* was coined by Wilhelm Ostwald (Fig. 1) when he considered systematically the different modes by which energy can be introduced into a

[a] *Institute of Nanotechnology, Karlsruhe Institute of Technology (KIT), Hermann-von-Helmholtz-Platz 1, D-76344 Eggenstein-Leopoldshafen, Germany. E-mail: vladimir.sepelak@kit.edu; Fax: +49-721-60826368; Tel: +49-721-60828929*

[b] *Center for Solid State Chemistry and New Materials, Leibniz University Hannover, Callinstr. 3-3a, D-30167 Hannover, Germany. E-mail: heitjans@pci.uni-hannover.de; Fax: +49-511-7624009; Tel: +49-511-7623187*

[c] *Institute of Physical Chemistry and Electrochemistry, Leibniz University Hannover, Callinstr. 3-3a, D-30167 Hannover, Germany. E-mail: andre.duevel@pci.uni-hannover.de, heitjans@pci.uni-hannover.de; Fax: +49-511-7624009; Tel: +49-511-7623187*

[d] *Institute for Chemistry and Technology of Materials, Graz University of Technology, Stremayrgasse 9, A-8010 Graz, Austria. E-mail: wilkening@tugraz.at; Fax: +43-316-87332332; Tel: +43-316-87332330*

[e] *Institute of Physical and Theoretical Chemistry, Braunschweig University of Technology, Hans-Sommer-Str. 10, D-38106 Braunschweig, Germany. E-mail: k-d.becker@tu-braunschweig.de; Fax: +49-531-3917305; Tel: +49-531-3915341*

† On leave from the Slovak Academy of Sciences, Košice, Slovakia.

system in order to induce or promote chemical changes.[6] He understood mechanochemistry as a part of physical chemistry like thermochemistry, electrochemistry, sonochemistry or photochemistry. It took, however, many more years until the presently accepted definition of mechanochemistry was given by Gerhard Heinicke in 1984 as "*Mechanochemistry is that branch of chemistry which is concerned with the chemical and physical changes of solids which are induced by the action of mechanical influences*".[7]

The present tutorial review is restricted to the mechanochemical phenomena in oxides, where an external mechanical force is technically exerted by high-energy ball milling or

Vladimir Šepelák

Vladimir Šepelák received his Diploma in Solid State Physics from P. J. Šafárik University in Košice (Slovakia), his PhD degree in Solid State Chemistry from Russian Academy of Sciences in Novosibirsk (Russia), and his habilitation in Materials Science from Technical University of Košice. He was an Alexander von Humboldt Fellow at Braunschweig University of Technology (Germany) and acted as a Mercator Professor of the German Research Foundation (DFG) at Leibniz University Hannover (Germany). Presently, he is affiliated with the Institute of Nanotechnology of the Karlsruhe Institute of Technology (KIT), and with the Slovak Academy of Sciences, Košice. His research interests include solid state chemistry, mechanochemistry, solid state physics, nanomagnetism, correlations between the local structure and functional behaviour of nanocrystalline solids, and spectroscopy of nonequilibrium phases.

Andre Düvel

Andre Düvel received his MSc in Chemistry from Leibniz University Hannover in 2009 and is currently pursuing his PhD degree in Physical Chemistry under the supervision of Paul Heitjans at the same place. His current research interests focus on the mechanochemical preparation of (metastable) fluorides and oxides and on the investigation of their (micro-)structural and ion conducting properties by employing solid state NMR and impedance spectroscopy.

Martin Wilkening

Martin Wilkening studied Chemistry at Leibniz University Hannover and obtained his doctoral degree (Dr rer. nat., with distinction) under the supervision of Paul Heitjans in 2005 with a dissertation on "Ultraslow Li Motions in Solids". His PhD thesis was awarded the Starck-Promotionspreis of the German Chemical Society (GDCh) and the Wissenschaftspreis Hannover. In 2011 he was appointed Full Professor at Graz University of Technology (Austria) and obtained the 'venia docendi' in solid state chemistry. In 2012 he received the 'venia legendi' (physical chemistry) from Leibniz University Hannover. For the thesis of his habilitation (qualification as a university lecturer in Germany and Austria) he obtained the ADUC annual award of the GDCh. In his workgroup, lithium and fluorine ion dynamics in solids are studied by NMR and impedance spectroscopy. In particular, his research focuses on nanostructured and amorphous energy materials including mechanosynthesized non-equilibrium compounds.

Klaus-Dieter Becker

Klaus-Dieter Becker is currently a Niedersachsen Professor at Braunschweig University of Technology. He received his Diploma and PhD degrees in Physics from Georg-August Universität Göttingen and his habilitation in Physical Chemistry from Ruhr-Universität Bochum (Germany). In 1995 he became a Full Professor of Physical Chemistry at Braunschweig University of Technology. His research interests are focused on the study of the solid state reactivity of bulk and nanomaterials mainly using spectroscopic techniques, e.g., Mössbauer and optical spectroscopy, applied under in situ conditions.

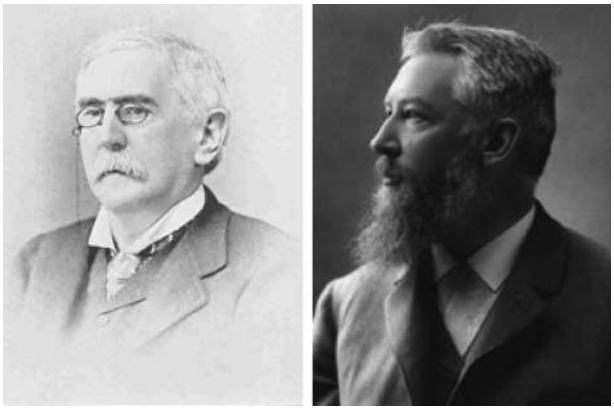

Fig. 1 (left) Matthew Carey Lea (1823–1897) established mechanochemistry as a separate branch of chemistry. (right) Wilhelm Ostwald (1853–1932) introduced the term mechanochemistry into the literature. Reproduced with permission from ref. 3, copyright 2005 Wiley-VCH Verlag GmbH & Co. KGaA, Weinheim.

Fig. 2 (a) A high-energy ball mill ''Pulverisette 7'' (Fritsch, Idar-Oberstein, Germany) of the planetary type and (b) a SPEX 8000M shaker mill (Spex CertiPrep Inc., USA) of the vibratory type, often used nowadays for the mechanochemical preparation of nanopowders.

grinding of the material. It should be noted that milling is one of the oldest technical activities of mankind which began with the use of stones to shell cereals, to break nuts or to crush food. Pestles and mortars were used in prehistoric times and the technique evolved continuously from the use of these primitive tools to that of milling equipment of modern times. The real metamorphosis of the applications of milling techniques into a true field of materials science occurred primarily during the second half of the twentieth century; the neologism *mechanical alloying* was proposed in the United States by a patent attorney in connection with the preparation of oxide-dispersed strengthened alloys by the high-energy ball milling technique.[8] Nowadays, milling is considered to be a mature technique used for the size reduction of solid particles even to the nanometer range, for the mixing and combination of chemical elements down to the atomic scale, and for the initiation or acceleration of solid state chemical reactions. Fig. 2 shows mechanochemical reactors often used nowadays for these purposes.

Mechanochemistry is well established in chemistry and materials science and has developed into a broad field, see ref. 9–21 for some recent reviews. New aspects of this field have emerged from recent developments in nanosciences. With atomic force and scanning tunneling microscopy techniques it is meanwhile possible to manipulate single molecules and to eventually induce chemical reactions.[20] Interestingly, the term mechanochemistry has recently also been introduced in quantum molecular dynamics simulations of the pulling of gold nanowires in atomic force microscopy.[21] *The Institute of Solid State Chemistry and Mechanochemistry* in Novosibirsk, Russia, founded as a Chemical and Metallurgical Institute in 1944, has carried its current name since 1997.[22] The *International Mechanochemical Association (IMA)* under the auspices of the International Union of Pure and Applied Chemistry (IUPAC) initiated the *International Conference on Mechanochemistry and Mechanical Alloying (INCOME)*,[23,24] which was held seven times since 1993, with the last meeting in Herceg Novi, Montenegro, in 2011. The recent IUPAC Compendium of Chemical Terminology defines a mechanochemical reaction as a ''*chemical reaction that is induced by the direct absorption of mechanical energy*''.[25]

Paul Heitjans

Paul Heitjans received his MSc and PhD degrees in Physics from Heidelberg University and his habilitation from Marburg University (Germany). Being delegated by these universities, he spent several years as a principal research scientist at Institute Laue-Langevin in Grenoble (France), and Research Center Jülich (Germany). In 1987 he became a Professor of Physical Chemistry at Leibniz University Hannover. He is also the founder and head of ZFM – Research Center for Solid State Chemistry and New Materials at Leibniz University Hannover. He was an invited professor at the Universities of Aberdeen (UK), Aberystwyth (UK), Newcastle (Australia) and Marseille (France). His research includes the development and application of solid-state NMR techniques as well as impedance spectroscopy to study mainly ion dynamics and transport in both solid-state model systems (emphasizing fundamentals) and functional materials (e.g., for Li ion batteries). Additionally, since more than ten years he and his group have been active in mechanochemistry research.

2. Mechanochemical reactions in oxides

In this review, which by no means exhausts the field of mechanochemistry, we shall focus on mechanochemical reactions in oxides and on their mechanically induced morphological, structural and compositional changes. Selected examples of functional properties, metastability and a high

reactivity of mechanosynthesized oxides shall be briefly demonstrated. As minerals, oxides belong not only to the most abundant phases of the Earth's crust and upper mantle but they constitute on their own a class of materials which are of tremendous scientific and technological importance.[26] Indeed, they display a rich variety of behaviours, some of which being not yet accounted for by theories accepted unanimously. For instance, this holds true for the high-temperature superconducting properties of some families of oxides.[27] Various properties of oxides are often combined to yield unique functional (*e.g.*, multiferroic) or structural materials.[28]

High-energy ball milling induces a variety of transformations and reactions in oxides such as disordering and amorphization (including surface amorphization), grain boundary disordering, polymorphic transformations, and so forth. It also creates defects, some being specific to oxides, such as Schottky or Frenkel defects or crystallographic shear planes (Wadsley defects). The chemical reactions in oxides induced by mechanical action can be categorized along the same lines that are commonly used in solid state chemistry and in chemistry, in general; they are either of *homogeneous* or of *heterogeneous* type.[5,13,29] Homogeneous processes shall be exemplified here by the mechanically triggered formation of nonequilibrium structural (atomic) and magnetic (spin) configurations in complex oxides and by mechanically induced phase transformations in binary oxides. Heterogeneous processes shall be illustrated with the specific case of mechanically induced formation reactions (the so-called *mechanochemical syntheses* or *mechanosyntheses*) of complex oxides.

2.1 Internal mechanochemical reactions: mechanically induced order–disorder reactions and phase transformations in oxides

The *homogeneous mechanochemical processes* considered in this section are confined to materials possibly consisting of different polymorphs but with a stationary chemical composition. Possible contaminations by elements from the milling tools or from the milling atmosphere are assumed to have negligible effects. These processes are due to the so-called "*mechanical activation*"[30] or "*mechanical grinding*".[5] Thus, in the following, we will present a series of examples of homogeneous mechanochemical reactions in which nanosized particles are produced by high-energy ball milling of a bulk oxide material (*top-down approach*). The nature of responses of oxides to mechanical action will be highlighted by examples focusing on

(a) the mechanically induced redistribution of cations over non-equivalent cation sublattices provided by a complex oxide structure,

(b) the formation of canted spin arrangements in the case of magnetic compounds,

(c) the changes in the geometry of constitutive polyhedra,

(d) the mechanically triggered formation of defective cation centers with an unsaturated oxygen coordination in the near-surface layers of oxide nanoparticles, and

(e) the mechanically induced phase transformation in oxides.

During the high-energy ball milling process, oxides are subjected to a continuous fragmentation accompanied by the reduction of their crystallite size (D) to the nanometer range. By this *comminution* many nanocrystalline materials were prepared which, in particular in the case of lithium containing complex oxides, show greatly enhanced (Li) ionic conductivity.[31,32] It should be emphasized that nanostructured oxides, in general, and especially those prepared by mechanochemical processing exhibit a high volume fraction of structurally disordered regions. As shown in Fig. 3, such nanostructures possess the so-called *core–shell* configuration consisting of ordered inner cores (often called *nanocrystalline grains* or *crystallites*) separated/surrounded by structurally disordered *internal interfaces* (grain boundaries) and *external surfaces* (near-surface layers).[33–35] Because of their sensitivity to medium- and long-range structural order, diffraction techniques lose much of their resolving power in such nanoscale and disordered systems. Spectroscopic techniques, such as magic angle spinning (MAS) nuclear magnetic resonance (NMR), Raman spectroscopy, X-ray photoelectron spectroscopy (XPS), and Mössbauer spectroscopy are efficiently applied to characterize these materials down to the atomic level.

Among structures susceptible to mechanical forces, complex oxides with the *spinel* structure exhibit a wide range of responses. These materials have been considered as convenient model systems for the investigation of mechanically induced processes in ionic systems because of their structural flexibility providing a wide range of physical and chemical behaviour.[13] 2–3 spinels of the type $M1^{2+}M2_2^{3+}O_4$, 2–4 spinels $M2_2^{2+}M1^{4+}O_4$

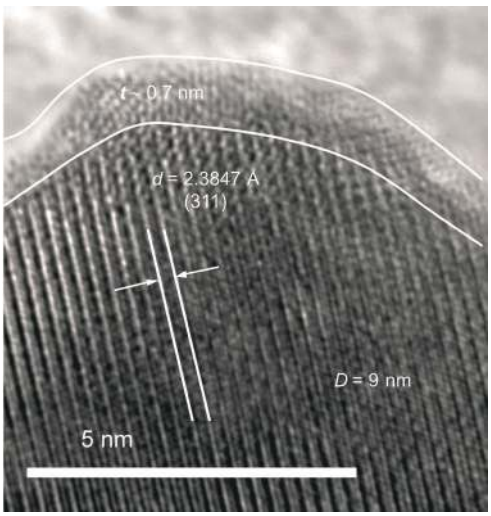

Fig. 3 High-resolution TEM micrograph of milled $Li_{0.5}Al_{2.5}O_4$ demonstrates the inhomogeneous structure of the produced nanoparticles with the size D = 9 nm which exhibit a clearly defined rim region and a core region. The so-called *core–shell* configuration of nanoparticles with the thickness t of the surface shell of about 0.7 nm is evident. The lattice fringes correspond to the crystallographic plane (311) (d = 2.3847 Å) of the $Li_{0.5}Al_{2.5}O_4$ phase (JCPDS PDF 38-1425). Reproduced with permission from ref. 34, copyright 2011 The Royal Society of Chemistry.

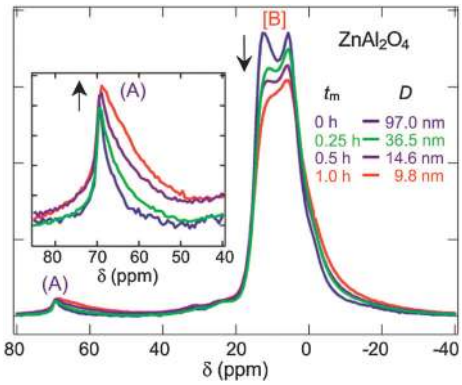

Fig. 4 ^{27}Al MAS NMR spectra of $ZnAl_2O_4$ milled various times. The milling times (t_m) and the corresponding crystallite sizes (D) are shown in the figure. Arrows emphasize the redistribution of the (A) and [B] spectral intensities. The inset shows the broadening and the increase in the intensity of the (A) subspectrum. Reproduced with permission from ref. 34, copyright 2011 The Royal Society of Chemistry.

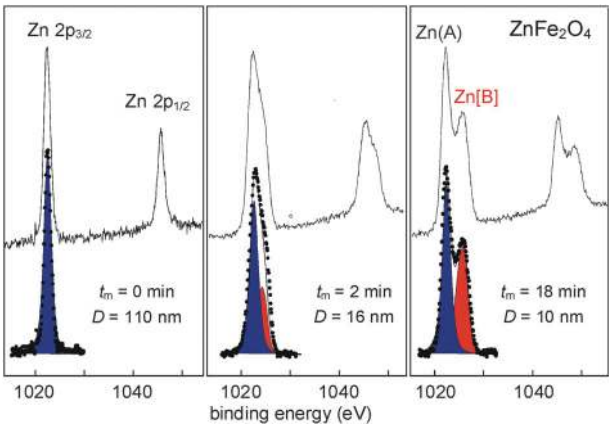

Fig. 5 XPS spectra of $ZnFe_2O_4$ milled various times in a planetary ball mill AGO 2 (product of the Institute of Solid State Chemistry and Mechanochemistry, Novosibirsk). The milling times and the corresponding crystallite sizes are shown in the figure. Adapted with permission from ref. 40, copyright 1999 Academic Press.

and 1–3 spinels $M1^{1+}_{0.5}M2^{3+}_{2.5}$ (where 2–3, 2–4 and 1–3 refer to the valences of the constituent cations) were found to exhibit complex disordering phenomena involving the redistribution of cations over the sites of tetrahedral (A) and octahedral [B] coordination provided by the spinel structure.[34–42] To emphasize the site occupancy at the atomic level, the structural formulae of these complex oxides may be written as $(M1_{1-\lambda}M2_{\lambda})[M1_{\lambda}M2_{2-\lambda}]O_4$ (for 2–3 and 2–4 spinels) and $(M1_{1-\lambda}M2_{\lambda})[M1_{\lambda-0.5}M2_{2.5-\lambda}]O_4$ (for 1–3 spinels), where parentheses and square brackets enclose cations on (A) and [B] sites, respectively. The symbol λ represents the so-called *degree of inversion* defined as the fraction of the (A) sites occupied by M2 cations. For 2–3 and 2–4 spinels, it varies from $\lambda = 0$ (*normal* spinel) to $\lambda = 1$ (*fully inverse* spinel), whereas λ takes a value from 0.5 to 1 in the case of 1–3 spinels. The values of $\lambda_{rd} = 2/3$ and $\lambda_{rd} = 5/6$ correspond to the random arrangement of cations in 2–3, 2–4 and 1–3 spinels, respectively.

Fig. 4 shows ^{27}Al MAS NMR spectra of the $ZnAl_2O_4$ spinel milled for various times (t_m) in a SPEX 8000M shaker mill.[34] Independent of the crystallite size, the NMR spectra of $ZnAl_2O_4$ consist of two well-resolved peaks in the region characteristic of tetrahedrally coordinated aluminium, Al^{3+}(A), (chemical shift $\delta \approx 70$ ppm; referenced to $Al(NO_3)_3$) and octahedrally coordinated aluminium, Al^{3+}[B], ($\delta \approx 8$ ppm). A signal with very low intensity is visible at approximately 35 ppm corresponding to a small amount of Al ions fivefold coordinated by oxygen. From the intensity ratio of the (A) and [B] spectral components ($I_{(A)}/I_{[B]}$) one can deduce quantitative information on the cation distribution in the material.‡ The degree of inversion of bulk $ZnAl_2O_4$ ($D \approx 97$ nm) is found to be $\lambda_c = 0.02(1)$. This indicates that the non-treated $ZnAl_2O_4$ is an almost *normal* spinel with the crystal chemical formula of $(Zn)[Al_2]O_4$. It is clearly visible that mechanical action on $ZnAl_2O_4$ results in a redistribution of the intensities of the (A) and [B] spectral lines. This reflects a decrease in the concentration of Al^{3+} cations on [B] sites and, *vice versa*, an increase in the population of Al^{3+} ions on (A) sites. The important observation is that the degree of inversion of $ZnAl_2O_4$ increases monotonically with decreasing D reaching $\lambda = 0.12(1)$ for crystallites with an average diameter of approximately 10 nm. Thus, mechanical action on $ZnAl_2O_4$ induces a homogeneous mechanochemical reaction yielding a nonequilibrium cation distribution which can be quantitatively formulated as: $(Zn_{0.98}Al_{0.02})[Zn_{0.02}Al_{1.98}]O_4$ ($\lambda_c = 0.02$) → $(Zn_{0.88}Al_{0.12})[Zn_{0.12}Al_{1.88}]O_4$ ($\lambda = 0.12$).

X-ray photoelectron spectroscopy, as a powerful surface analytical method, was applied to follow the homogeneous mechanochemical processes at the atomic level in the $ZnFe_2O_4$ spinel.[40] As seen in Fig. 5, the Zn $2p_{3/2}$ signal of bulk (unmilled) $ZnFe_2O_4$ consists of a single sharp peak located at 1021.8 eV, which corresponds to the tetrahedrally coordinated zinc ions. This indicates that bulk $ZnFe_2O_4$ adopts the *normal* spinel structure ($\lambda_c = 0$). With increasing t_m (with decreasing D), the XPS signal becomes broader, and a new spectral component gradually appears on its high-energy side (at 1023.2 eV) corresponding to octahedrally coordinated zinc. The new spectral component is clearly visible in the XPS spectrum of $ZnFe_2O_4$ already after 2 min of milling. After relatively short t_m (18 min), the population of Zn^{2+} cations on [B] sites reaches the value of $\lambda = 0.41(2)$. Thus, in contrast to the bulk material, milled nanocrystalline $ZnFe_2O_4$ exhibits a *partly inverse* spinel structure characterized by a far-from-equilibrium cation distribution. This observation is consistent with the results of EXAFS investigations of milled Zn-containing nanospinels.[41] Quantitatively, the homogeneous mechanochemical process of cation redistribution in $ZnFe_2O_4$ can be written as $(Zn)[Fe_2]O_4$ ($\lambda_c = 0$) → $(Zn_{0.59}Fe_{0.41})[Zn_{0.41}Fe_{1.59}]O_4$ ($\lambda = 0.41$). As the mean free path of photoelectrons in zinc oxides is about 2 nm, XPS measurements give information on a depth of about 6 nm.[40] It should be emphasized that as the particle size of milled $ZnFe_2O_4$ is $D \approx 10$ nm, the results of the XPS measurements reflect not

‡ $\lambda = 2I_{(A)}/(I_{(A)} + I_{[B]})$ and $\lambda = 2.5I_{(A)}/(I_{(A)} + I_{[B]})$ for 2–3, 2–4 and 1–3 spinels, respectively.

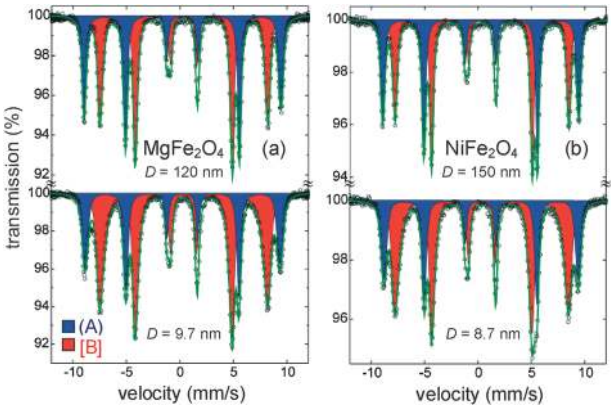

Fig. 6 Low-temperature (6.4 K) ^{57}Fe Mössbauer spectra of bulk and nanocrystalline (a) $MgFe_2O_4$ and (b) $NiFe_2O_4$. The nanoferrites were prepared by high-energy ball milling the corresponding bulk materials in a planetary ball mill EI 2 × 150 (product of the Institute of Solid State Chemistry and Mechanochemistry, Novosibirsk). The spectra with the completely resolved (A) and [B] subspectra were taken in an external magnetic field of 5.5 T applied perpendicular to the γ-ray direction. Modified with permission from ref. 37 (a), copyright 2000 American Institute of Physics. Adapted with permission from ref. 42 (b), copyright 2002 Elsevier Science B.V.

only the structure of the near-surface layers but also the disorder in the interior of the $ZnFe_2O_4$ nanoparticles.

Low-temperature ^{57}Fe Mössbauer measurements in a large external magnetic field allow an accurate determination of the cation distribution in mechanically treated spinel ferrites.[29,36–38,42] This is because the subspectra corresponding to Fe cations on (A) and [B] sites, which overlap in the zero field, become separated in large external magnetic fields. Further, Mössbauer spectra recorded at low temperatures are easier to interpret because of the absence of magnetic relaxation effects (*e.g.*, superparamagnetism) associated with the nanoscale nature of milled magnetics.[33] It is found that mechanochemical processing of *inverse* spinel ferrites is, in contrast to *normal* spinels, accompanied by a decrease in the concentration of Fe^{3+} cations on (A) sites, *i.e.*, by a decrease in the degree of inversion. This is clearly demonstrated in Fig. 6, where the low-temperature (6.4 K) in-field (5.5 T) ^{57}Fe Mössbauer spectra of the mechanically prepared nanocrystalline spinels $MgFe_2O_4$ and $NiFe_2O_4$ are compared with those of the corresponding bulk counterparts. It is revealed that the non-treated $MgFe_2O_4$ and $NiFe_2O_4$ adopt a *partly inverse* and a *fully inverse* spinel structure of the type $(Mg_{0.10}Fe_{0.90})[Mg_{0.90}Fe_{1.10}]O_4$ (λ_c = 0.90) and $(Fe)[NiFe]O_4$ (λ_c = 1.00), respectively, whereas the degree of inversion of the nanosized ferrites is found to be $\lambda \approx 0.7$.[37,38,42]

In addition to the information about local coordination and the charge of iron ions, ^{57}Fe Mössbauer spectroscopy offers a unique possibility of studying the spin arrangement in a magnetic sample.[37,38] When an external magnetic field is applied perpendicularly to the γ-ray direction, the average spin canting angle, Ψ, can easily be calculated from the ratio of the intensities of lines 2 and 1, I_2/I_1, of the magnetically split six-line spectra.§ For example, for bulk $MgFe_2O_4$ and $NiFe_2O_4$ (Fig. 6), the intensity ratio I_2/I_1 is found to be about 4/3. It is concluded that the spins are aligned with the external magnetic field of 5.5 T, *i.e.*, the bulk ferrites exhibit a Néel collinear spin arrangement of the type $(Mg_{0.1}Fe_{0.9}\uparrow)[Mg_{0.9}Fe_{1.1}\downarrow]O_4$ and $(Fe\uparrow)[Ni\downarrow Fe\downarrow]O_4$. The degree of noncollinearity of the spins increases with increasing t_m of the ferrites, *i.e.*, with decreasing D.[37,38] The average spin canting angles were found to be $\Psi \approx 24^\circ$ and $\Psi \approx 26^\circ$ for nanocrystalline ($D < 10$ nm) $MgFe_2O_4$ and $NiFe_2O_4$, respectively. Thus, in addition to the cation disorder, nanoscale magnetic oxides prepared by mechanochemical routes exhibit magnetic disorder owing to *spin canting*.

Another interesting feature observed is that mechanical action on spinel oxides brings about a noticeable broadening of the (A) and [B] spectral lines (compare the NMR, XPS and Mössbauer spectra in Fig. 4–6), which implies a change in the local atomic environments around the (A)- and [B]-site cations. This variation is explained to be a consequence of the mechanically induced *deformation of polyhedron geometries*, *i.e.*, the presence of distorted oxygen tetrahedra and octahedra.[34,37]

The change in cationic order in spinels is usually induced by high temperature,[43] high pressure,[44] and irradiation of a material with high-energy electrons, ions or neutrons.[45] All of these processing parameters were found to change the cation distribution in spinels towards random arrangement ($\lambda \rightarrow \lambda_{rd}$). The examples given above clearly show that mechanical action has the same randomizing influence on the cation distributions (Fig. 7).[35] Note that it holds for nearly *normal* spinels with a low degree of inversion – where λ increases due to milling – as well as for nearly *inverse* spinels with their starting bulk values close to λ = 1 – in which λ decreases during high-energy ball milling.

Even though we are aware that it is not feasible to formally transfer the processes establishing the equilibrium distribution of cations, taking place during thermal "activation", to the case of

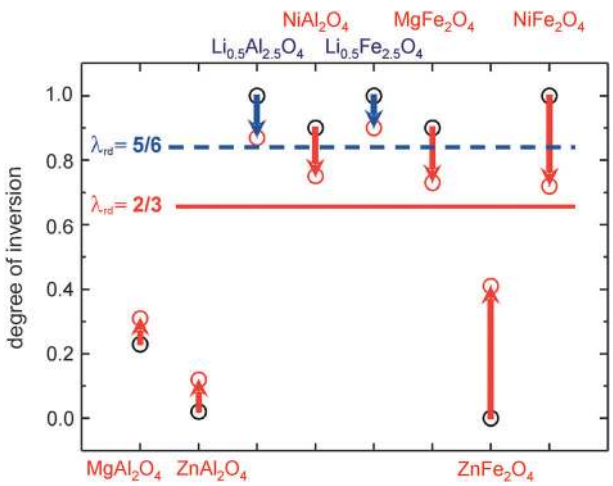

Fig. 7 Cation distributions in spinels and their changes upon high-energy ball milling. Independently of the ionic configuration in non-treated spinels, mechanical action is found to change their cation distributions towards the random arrangement ($\lambda \rightarrow \lambda_{rd}$; λ_{rd} = 2/3 and 5/6 for 2–3 and 1–3 spinels, respectively). Reproduced with permission from ref. 35, copyright 2012 The Korean Ceramic Society.

§ $\Psi = 90^\circ - \arcsin\{[3(I_2/I_1)/2]/[1 + 3(I_2/I_1)/4]\}^{1/2}$. Lines counted from left to right.

mechanical ''activation'', the efficiency of mechanochemical methods can be documented by the fact that the degree of inversion reached in nanosized milled spinels corresponds to that of the bulk oxides thermally treated at about 2000 K.[39] Taking into account the impact-induced local heating and high local pressures (sometimes called ''hot spots'' or ''thermal spikes'')[7,46] involved in the high-energy ball milling process, the mechanically induced order–disorder reactions presented above could be understood to occur at the moment of impact as a result of formation and freezing-in of high-energy localized states.

Taking into account the non-uniform core–shell configuration of the milled oxides (see Fig. 3), their λ values determined by spectroscopic techniques can be considered as mean values reflecting the cation distribution within their ordered grains and disordered interfaces/surfaces. The atomic configurations in the interface/surface regions of spinel oxides prepared by mechanochemical routes are chiefly characterized by a nearly *random* arrangement of cations (λ_{rd}),[47,48] see below. In contrast, the ordered grains of nanooxides were found to exhibit an equilibrium cation distribution (λ_c). Thus, the experimentally determined λ values for the milled oxides can be expressed as $\lambda = (1 - w)\lambda_c + w\lambda_{rd}$, where w is the volume fraction of interfaces/surfaces. Assuming a spherical shape of the as-prepared oxide nanoparticles, the volume fraction of interfaces/surfaces and their thickness (t) can be estimated using the experimentally determined λ, λ_c and D values.¶ It can be seen (Table 1) that the volume fraction of the structurally disordered interface/surface regions in the spinel nanooxides of comparable crystallite size ($D \approx 10$ nm) ranges from about 16% to 64%. On average, the w values for relatively brittle spinel aluminates are found to be smaller than those observed in the mechanochemically prepared spinel ferrites.[5,34] Generally, the latter are more ductile materials. Consequently, various t values observed for the investigated spinels may also be related to their different resistivity with respect to mechanical action (to their different mechanical properties). We note that, in general, 1 nm is a typical thickness of grain boundary/surface shell regions in nanostructured mechanochemically prepared oxides, such as cubic spinels,[47–50] olivines,[26] perovskites,[28] as well as orthorhombic and ilmenite-type complex oxides.[51–53] In contrast to spinel nanooxides, whose near-surface layers are disordered due to the random distribution of cations, the canted spin arrangement (in the case of magnetic oxides), as well as deformed polyhedra,[49,50] in the case of mechanosynthesized perovskites (*e.g.*, $BiFeO_3$) and trigonal nanocrystalline oxides (*e.g.*, $LiNbO_3$), the surface shell regions have been found to be even amorphous.[28,53]

A second learning example for *homogeneous mechanochemical reactions* is that of mechanically induced phase transformations in oxides. It has been shown that the occurrence of polymorphic transformations in oxides upon high-energy ball milling, and their kinetics, depends chiefly on dynamical conditions of the milling process.[5] For example, highly energetic conditions are needed to induce the phase transformation of γ-Al_2O_3 into the thermodynamically stable α-Al_2O_3. ^{27}Al MAS NMR spectroscopy carried out at a very high magnetic field of 17.6 T allowed a systematic investigation of this transformation from an atomic scale point of view.[54] The study revealed that unsaturated Al ions, *i.e.*, those ions coordinated fivefold by oxygen (in the following denoted as AlO_5), are formed to an unexpectedly large fraction as high as 20% (Fig. 8a). These *defective cation centers with an unsaturated oxygen coordination* are found to be crucial

Table 1 The volume fraction of interfaces/surfaces (w) and their average thickness (t) in nanocrystalline spinel oxides estimated using the experimentally determined mean degree of inversion (λ) and the average crystallite diameter (D). The observed λ results from two contributions: that of nanosized crystallites which possess a cation ordered bulk-like structure characterized by the degree of inversion λ_c, and that of disordered interfaces/surfaces with a random distribution of cations (λ_{rd}). The data for aluminates and ferrites are reproduced with permission from ref. 5 (copyright 2011 The Royal Society of Chemistry) and ref. 34 (copyright 2012 The Royal Society of Chemistry), respectively

Oxide	D (nm)	λ	λ_c	λ_{rd}	w (%)	t (nm)
$ZnAl_2O_4$	9.8(2)	0.12(1)	0.02(1)	2/3	15.5(3)	0.3(1)
$MgAl_2O_4$	8.1(3)	0.31(1)	0.23(1)	2/3	18.3(4)	0.3(1)
$Li_{0.5}Al_{2.5}O_4$	9.6(4)	0.94(1)	1.00(1)	5/6	36.0(4)	0.7(1)
$MgFe_2O_4$	9.7(1)	0.75(6)	0.90(4)	2/3	64.2(8)	1.4(1)
$ZnFe_2O_4$	10.0(1)	0.41(2)	0	2/3	61.5(1)	1.3(2)

¶ $w = 100[(\lambda - \lambda_c)/(\lambda_{rd} - \lambda_c)]$; $t = D/2 - [(D/2)^3(100 - w)/100]^{1/3}$.

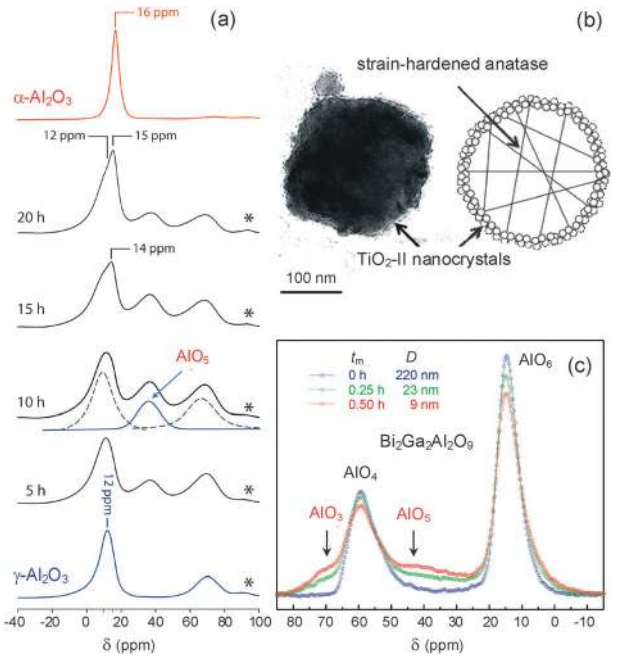

Fig. 8 (a) ^{27}Al MAS NMR spectra demonstrate the phase transformation of γ-Al_2O_3 into α-Al_2O_3 induced by high-energy ball milling in a Pulverisette 7 planetary mill. The milling times are indicated. Adapted with permission from ref. 54, copyright 2011 American Chemical Society. (b) (left) TEM micrograph of titania powder ground for 5 min. (right) Schematic drawing showing nanosized TiO_2-II crystallites formed on the surface of the milled anatase particles. Adapted with permission from ref. 5, copyright 2012 The Royal Society of Chemistry. (c) ^{27}Al MAS NMR spectra of $Bi_2Ga_2Al_2O_9$ milled various times in a Pulverisette 7 planetary mill. Arrows denote the spectral components corresponding to the anomalous AlO_5 and AlO_3 nearest-neighbor atomic configurations. Adapted with permission from ref. 5, copyright 2012 The Royal Society of Chemistry.

for the phase transformation induced by mechanical treatment indicating that the reaction mechanism is similar to that reported for the thermally induced $\gamma \rightarrow \alpha$ phase transformation, *i.e.*, the growth of α-Al_2O_3 starts from the unsaturated Al centers on the, presumably structurally disordered, surface of a metastable γ-Al_2O_3 crystallite and propagates into the inner regions. Furthermore, it turned out that the presence of α-Al_2O_3 seed crystals seems to play neither the major nor the only role in initializing the phase transformation. The main reason for a complete phase transformation has to be looked for in the very early stages of milling. Obviously, the initial surface area of the starting material takes a decisive part; the smaller the surface area of the crystallites the easier the phase transformation takes place. Presumably, this is due to the fact that the γ-modification of Al_2O_3 becomes stabilized when the mean crystallite size falls below a certain limit.[54]

From numerous reports in the literature,[5] the following examples of mechanically induced phase transformations in binary oxides shall be mentioned: the anatase modification of TiO_2 was reported to transform by high-energy milling into the rutile polymorph *via* the so-called TiO_2-II phase (high-pressure polymorph with an α-PbO_2-type structure). TiO_2-II crystallites with diameters around 10 nm were observed to form on the surface of the milled anatase particles (Fig. 8b). The thickness of the superficial TiO_2-II layer surrounding a strain-hardened core of anatase particles was found to increase with milling time t_m. In the case when cubic Y_2O_3 possessing a bixbyite type structure is milled, a monoclinic modification of Y_2O_3 (stable at high temperatures and at high pressures under equilibrium conditions) appears first while an amorphous phase is observed to form after prolonged milling. Similarly, the cubic polymorphs of Dy_2O_3 and of Er_2O_3 may transform upon high-energy ball milling into their monoclinic forms. The monoclinic-to-tetragonal phase transition in ZrO_2 can also be induced by the high-energy milling process. Note that the transformation path (*i.e.*, the sequence of phases formed) during the milling of the above-mentioned binary oxides is the same as that induced thermally. It has been reported that plastic deformations play an important role in the occurrence of phase transformations during grinding. Moreover, an increase in local temperatures may be significant in oxide particles during shocks. The combined actions of increased defect concentrations and the impact-induced local heating enhance atomic mobility and may force phase transformations. The phase transformations of the ground oxides described above may also be related to the ability of their structural units (in general MO_6 octahedra) to rearrange themselves.[5]

One of the most important aspects of studies on mechanically induced phase transformations in oxides, performed up to date, is the exploration of simple routes to compounds with a large amount of *defective cation centers with an unsaturated oxygen coordination* (*e.g*, AlO_5) which can easily be adjusted by the milling time as well as the time and temperature of a subsequent annealing step.[54] Quite recently it was found that mechanical action on the mullite-type $Bi_2(Ga_2Al_2)O_9$ material gives birth to three- and fivefold coordinated Al centers (Fig. 8c).[5] The concentration of these defective AlO_3 and AlO_5 configurations increases with increasing t_m, reaching a value of about 21% in nanomaterials with crystallite sizes below 10 nm. The so prepared nanostructured oxides, which are in this case free of any additives, might be of large interest for the preparation of catalysts since the unsaturated Al centers act as anchoring sites for catalytically active materials.[55] Thus, the mechanical preparation route found might establish a basis for the design of catalysts whose activity can be thoroughly tailored. Finally, the investigations on the phase transformations upon milling clearly show that mechanochemical methods provide highly effective tools to create (metastable) compounds which are not available by conventional synthesis routes.[54]

2.2 Mechanosyntheses of complex oxides

It is widely appreciated that the performance of oxides and of materials, in general, is closely related to the ways in which they are processed. The conventional solid state (ceramic) synthesis of complex oxides requires a number of stages including homogenization of the powder precursors, compaction of the reactants, and finally their prolonged heat treatment at considerably high calcination temperatures. In many cases, this causes losses of constituent elements due to their high volatility and, consequently, it results in the formation of multiphase products and the degradation of microstructural and functional properties of oxide materials.[28,50] Various wet chemistry-based routes have also been developed to synthesize nanosized oxide powders. However, most of the solution chemistry-based routes still involve calcinations, although at relatively lower temperatures. One goal of modern chemistry research and materials development has been to identify simpler processing schemes that do not rely upon high-temperature treatments for inducing solid state reactions.[52] Among the many types of preparation techniques, the non-conventional mechanochemical processing has been recognized as an alternative route overcoming all of the above-mentioned problems and providing an efficient one-step and facile access to nanomaterials.[9–17]

The most important types of *heterogeneous mechanochemical processes* in oxides include formation reactions, decomposition reactions of compounds, and reduction–oxidation processes.[5,46] These processes comprise *multi-constituent* solid state systems. Mechanically induced formation reactions (mechanosyntheses) represent one of the major subjects of mechanochemistry.[9,14,17] The preparation of far-from-equilibrium and (simultaneously) nanostructured materials with unusual functional properties, markedly different from those of their micrometer-sized counterparts, provides a major source of motivation for mechanosynthesis.[17] This route, which includes several stages such as the mixing of precursors at the atomic level, the nucleation of a new product phase and its growth, can be considered as a *bottom-up approach* for the preparation of nanostructured materials.[5,17]

In this section, we shall exemplify the richness of heterogeneous mechanochemical processes by discussing the mechanosynthesis of different families of complex oxides (stannates, silicates, ferrites, lanthanates) with a variety of structure types

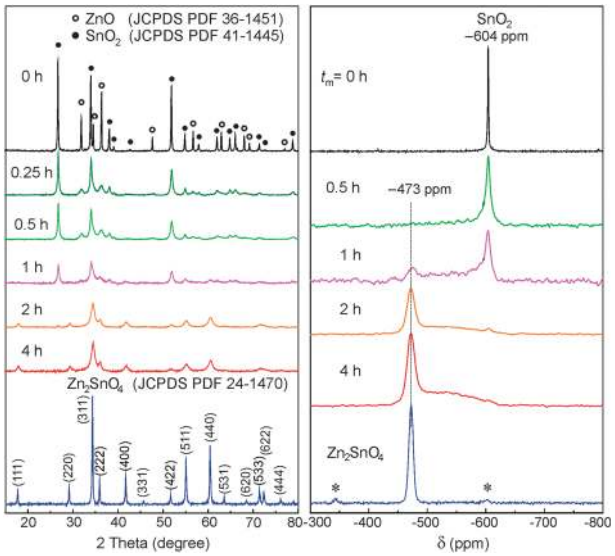

Fig. 9 (left) XRD patterns and (right) ^{119}Sn MAS NMR spectra of the 2ZnO + SnO_2 mixture milled various times (up to 4 h) and of (bottom) the bulk Zn_2SnO_4 prepared by the conventional ceramic route. The mechanosynthesis was performed in a Pulverisette 7 planetary mill. The milling times are shown in the figure. Diffraction peaks of the bulk Zn_2SnO_4 are denoted by Miller indices. Spinning sidebands associated with the resonance at −473 ppm are marked with *. Adapted with permission from ref. 50, copyright 2012 The Royal Society of Chemistry.

(spinel, olivine, perovskite, garnet). It shall be demonstrated that these oxides can be mechanosynthesized at ambient temperature directly from their precursors in the form of nanosized powders without the need for calcination at intermediate temperatures, thus making the process very simple and cost-effective.

Fig. 9 illustrates the mechanosynthesis of zinc stannate from a mixture of binary oxides ($2ZnO + SnO_2 \rightarrow Zn_2SnO_4$) followed by XRD and ^{119}Sn MAS NMR.[50] As can be clearly seen, in the XRD pattern of the mixture milled for 4 h, all diffraction peaks detected can be ascribed to the Zn_2SnO_4 phase. Similarly, after 4 h of milling, the resonance peak at −604 ppm (referenced to microcrystalline SnO_2), corresponding to the Sn atoms located in SnO_6 octahedra in the tetragonal structure of the SnO_2 educt, has disappeared completely. The corresponding NMR spectrum of the milled powder is dominated by the lines assigned to the Sn^{4+} cations in the spinel structure of mechanosynthesized Zn_2SnO_4.[50] For comparison, the XRD pattern and the NMR spectrum of the Zn_2SnO_4 reference sample (the bulk material prepared by the conventional ceramic route) are also presented at the bottom of Fig. 9. In contrast to relatively narrow XRD reflexes for the bulk Zn_2SnO_4, the broadened diffraction peaks of the mechanosynthesized stannate provide clear evidence of the nanoscale nature of the mechanosynthesized product.

It is well recognized that functional properties of nanostructured materials prepared by mechanochemical routes are determined to a large extent by their interfaces/surfaces (see Fig. 10).[33,47–52] Thus, a fundamental understanding of such "interface-controlled" materials relies on a careful separation of

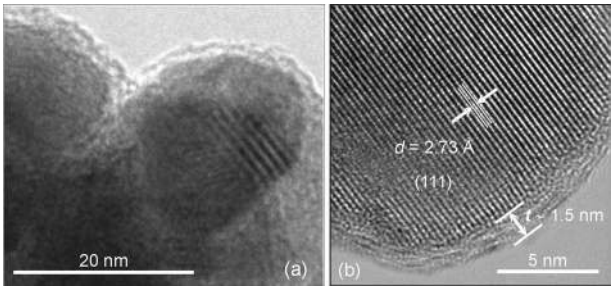

Fig. 10 (a) Bright-field and (b) high-resolution TEM images of mechanosynthesized Ca_2SnO_4. The core–shell configuration of mechanosynthesized nanoparticles with the thickness of the surface shell of about 1.5 nm is evident. The lattice fringes correspond to the crystallographic plane (111) (d = 2.73 Å) of the Ca_2SnO_4 phase (JCPDS PDF 46-0112). Adapted with permission from ref. 52, copyright 2009 American Chemical Society.

their surface and bulk effects. In the following, based on comparative spectroscopic studies of bulk samples being conventionally prepared and their nanosized mechanosynthesized counterparts, selected examples of the separation of surface effects from bulk effects in oxide nanoparticles will be presented.

In particular, the complementary methodological approach (*i.e.*, the application of a variety of spectroscopic techniques) allowed a systematic investigation of structural disorder at the atomic level within the core and shell of mechanosynthesized oxide nanoparticles.[26,28,40,46–52] For example, ^{119}Sn MAS NMR and Raman spectroscopy provided valuable complementary insights into the nature of the short-range structural disorder of the mechanosynthesized 2–4 spinel Zn_2SnO_4 (see Fig. 11).[50] The relatively narrow resonance line at −473 ppm (referenced to microcrystalline SnO_2) is ascribed to arise from Sn^{4+} cations

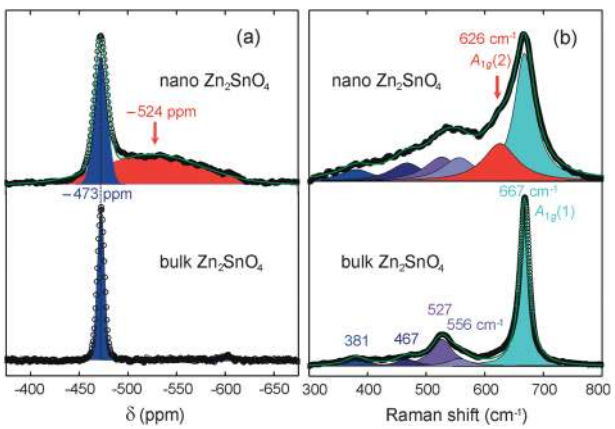

Fig. 11 (a) ^{119}Sn MAS NMR spectra and (b) Raman spectra of (top) mechanosynthesized nanoscale Zn_2SnO_4 and (bottom) bulk Zn_2SnO_4 prepared by the conventional thermal route. The resonance line at −473 ppm arises from the octahedrally coordinated Sn ions in the core of Zn_2SnO_4 nanoparticles, whereas the broad line centered at −524 ppm is associated with the Sn ions occupying deformed SnO_6 octahedra in the near-surface layers of nanoparticles. The frequencies of the Raman modes are indicated in the figure. The phonon band at 626 cm^{-1} is assigned to the vibrations of the Sn–O bonds in the SnO_4 tetrahedra created by the redistribution of some Sn ions from [B] to (A) sites. Adapted with permission from ref. 50, copyright 2012 The Royal Society of Chemistry.

located in regular SnO_6 octahedra in the core of Zn_2SnO_4 nanoparticles whereas the broad line centered at −524 ppm is associated with the Sn ions occupying highly distorted SnO_6 octahedra in the near-surface layers of the nanoparticles. Integration of the intensities of the NMR lines reveals that about 50% of the Sn atoms are located in the disordered surface shell of the as-prepared nanoparticles. Moreover, the phonon band at 626 cm^{-1}, observed exclusively in the Raman spectrum of the mechanosynthesized Zn_2SnO_4 spinel (Fig. 11b), is assigned to the fundamental Raman-active vibration of the Sn–O bonds in the SnO_4 tetrahedra created by the redistribution of some Sn ions from [B] to (A) sites. In other words, the Raman investigation of the stannates indicates that, in contrast to the bulk material exhibiting the *fully inverse* spinel structure of the type $(Zn)[SnZn]O_4$, the nanoscale mechanosynthesized Zn_2SnO_4 adopts a *partly inverse* spinel structure characterized by the crystal chemical formula $(Zn_\lambda Sn_{1-\lambda})[Sn_\lambda Zn_{2-\lambda}]O_4$. Thus, the comparative spectroscopic studies of bulk and nanocrystalline Zn_2SnO_4 enable us to separate surface effects from bulk effects in mechanosynthesized nanoparticles; the inner core of nanoparticles is found to possess the fully inverse spinel structure with the regular geometry of constitutive polyhedra whereas the surface shell is disordered due to a nonequilibrium cation distribution and a broadly distorted local environment around the cations.

The next example deals with the mechanosynthesis of calcium stannate ($2CaO + SnO_2 \rightarrow Ca_2SnO_4$) with an orthorhombic structure,[52] which was followed by ^{119}Sn MAS NMR and ^{119}Sn Mössbauer spectroscopy. The two spectroscopies are remarkably complementary in this case insofar as NMR spectroscopy is concerned with the nuclear ground state of ^{119}Sn nuclei which possess spin $I = 1/2$ and thus exclusively reflect chemical shift interactions experienced by the nuclei. On the other hand, Mössbauer spectroscopy involves transitions between the ground and first excited nuclear states (where the latter possesses spin $I = 3/2$) and therefore provides information on the quadrupolar interactions experienced by the nuclei of ^{119}Sn. In this context, the Ca_2SnO_4 formation reaction represents an excellent model system for studies of local structural changes during mechanosynthesis because the tin nucleus ^{119}Sn can serve as a local probe in both NMR and Mössbauer measurements. The broad shape of the NMR lines observed for the mechanosynthesized product, which is in contrast to the relatively narrow lines for the bulk stannates (Fig. 12a), implies the presence of broadly distributed local environments around the Sn nuclei due to the mechanically induced distortion of the SnO_6 octahedra. On the other hand, an interesting observation is that the average quadrupole splitting for mechanosynthesized Ca_2SnO_4 is significantly smaller than that estimated for the conventionally prepared stannate (see Fig. 12b). This reflects the presence of smaller electric field gradients acting on Sn nuclei in the nanocrystalline material. Consequently, this gives evidence of the presence of distorted but *more symmetric* SnO_6 octahedra in the mechanosynthesized stannate. This striking local structural feature has also been observed to occur in other mechanosynthesized complex oxides with the

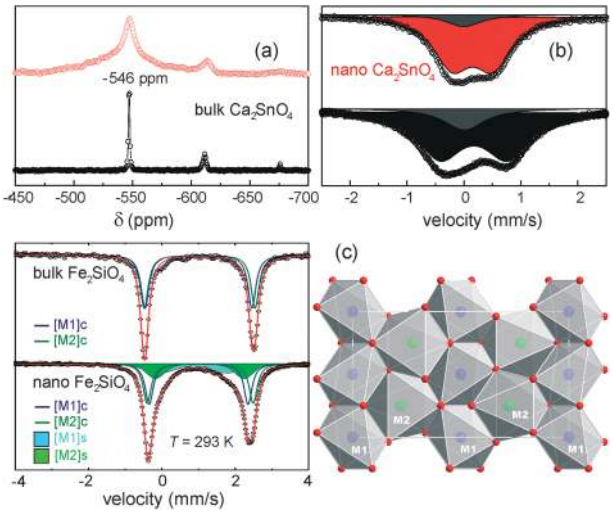

Fig. 12 (a) ^{119}Sn MAS NMR spectra and (b) ^{119}Sn Mössbauer spectra of (top) nanosized mechanosynthesized Ca_2SnO_4 and (bottom) bulk Ca_2SnO_4 prepared by the conventional thermal route. The mechanosynthesis was completed after 4 h of milling the mixture of precursors ($2CaO + SnO_2$) in a Pulverisette 6 planetary mill. Modified with permission from ref. 52, copyright 2009 American Chemical Society. (c) (left) Room-temperature ^{57}Fe Mössbauer spectra of bulk α-Fe_2SiO_4 and nanosized mechanosynthesized α-Fe_2SiO_4 with the olivine structure. The mechanosynthesis was completed after 4 h of milling the mixture of precursors (2α-$Fe_2O_3 + 2Fe + 3SiO_2$) in a Pulverisette 6 planetary mill. [M1]c, [M2]c and [M1]s, [M2]s denote cation sites of octahedral coordination in the inner core and the surface shell of α-Fe_2SiO_4 nanoparticles, respectively. (right) Schematic presentation of the olivine structure. Modified with permission from ref. 26, copyright 2012 The Royal Society of Chemistry.

orthorhombic structure such as fayalite (α-Fe_2SiO_4).[26] In the latter case, ^{57}Fe Mössbauer spectroscopy even allows a quantitative determination of the distribution of Fe^{2+} cations within the core (with regular and asymmetric octahedra) and shell (with distorted albeit more symmetric octahedra) of mechanosynthesized nanoparticles. Based on the results of ^{57}Fe Mössbauer analysis (Fig. 12c), the crystal chemical formula emphasizing the site occupancy at the atomic level in the nanofayalite can be represented as $[Fe_{0.6}]_{[M1]c}[Fe_{0.6}]_{[M2]c}$-$[Fe_{0.4}]_{[M1]s}[Fe_{0.4}]_{[M2]s}SiO_4$, where [M1]c, [M2]c and [M1]s, [M2]s denote cation sites of octahedral coordination in the inner core and the surface shell of α-Fe_2SiO_4 nanoparticles, respectively. Note that bulk fayalite crystallizes with the olivine structure of the type $[Fe]_{[M1]}[Fe]_{[M2]}SiO_4$.

In the case of the important group of mechanosynthesized iron-containing magnetic oxides such as spinel ferrites MFe_2O_4 (M = Mg, Ni, Mn, Zn),[47–49,56] their core–shell morphology requires to fit their ^{57}Fe Mössbauer spectra by a superposition of four spectral components (Fig. 13): two accounting for Fe^{3+} nuclei at (A) and [B] sites of the particle core and two associated with Fe^{3+} ions at (A) and [B] sites in the surface shell of the nanoparticles. Thus, it could be revealed that the surface shell of ferrite nanoparticles is structurally and magnetically disordered owing to the nearly random distribution of cations ($\lambda_s \approx 0.67$) and the canted spin arrangement ($\Psi_s \approx 28$–40°). This is in contrast to the cation ordered bulk-like core of the ferrite nanoparticles with a collinear spin alignment ($\Psi = 0^\circ$).[47,48]

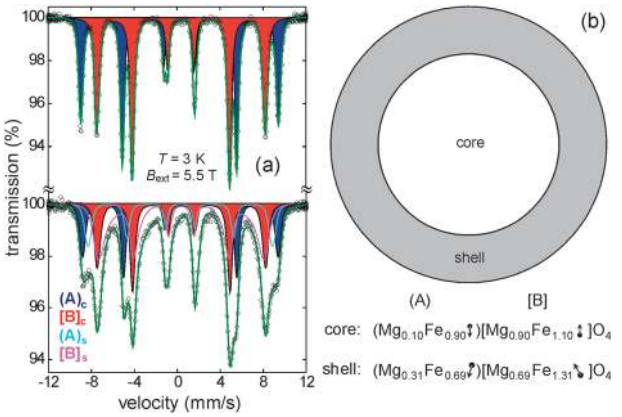

Fig. 13 (a) Mössbauer spectra of (top) bulk $MgFe_2O_4$ and (bottom) nanosized mechanosynthesized $MgFe_2O_4$ taken at 3 K in an external magnetic field of 5.5 T applied perpendicular to the γ-ray direction. $(A)_c$, $[B]_c$ and $(A)_s$, $[B]_s$ denote cation sites of tetrahedral and octahedral coordination in the inner core and the surface shell of $MgFe_2O_4$ nanoparticles, respectively. (b) Schematic drawing showing the non-uniform nanostructure of mechanosynthesized $MgFe_2O_4$. The crystal chemical formulae emphasize the spin alignment and the site occupancy at the atomic level within the particle core and shell. Modified with permission from ref. 47, copyright 2006 American Chemical Society.

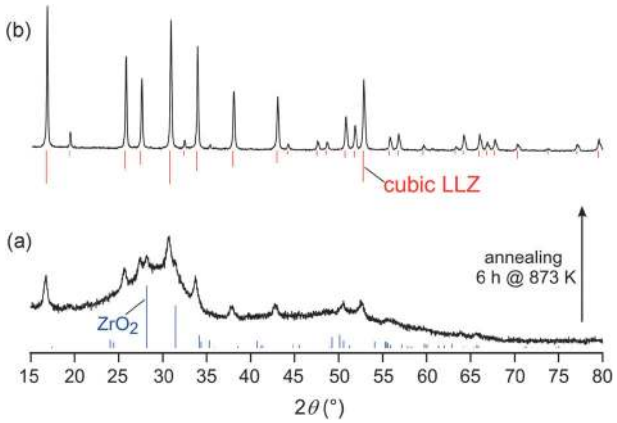

Fig. 14 XRD patterns demonstrating a combined mechanochemical-thermal route to Al-doped garnet-like $Li_7La_3Zr_2O_{12}$ with cubic structure. (a) XRD pattern of the material prepared by high-energy ball milling of a mixture of binary oxides (Li_2O, ZrO_2, Al_2O_3, La_2O_3) for 8 h in a Pulverisette 7 planetary mill. (b) XRD pattern of Al-doped cubic $Li_7La_3Zr_2O_{12}$ obtained after heat treatment of the material at 873 K for 6 h. Reproduced with permission from ref. 59, copyright 2012 American Chemical Society.

Clearly, such a far-from-equilibrium state confined to the particle's near-surface layers of the mechanosynthesized ferrites has significant implications for their magnetic behaviour. In this context it should be mentioned that both, the "magnetically active" surface shell, exhibiting a two times larger effective magnetic moment than bulk material,[47] as well as the "magnetically dead" surface shell (with zero effective magnetic moment)[48] have been reported for nanosized mechanosynthesized ferrites. These findings are consistently explained in terms of the so-called *modified core–shell model*,[57] in which a competition between the effects of spin canting and site exchange of cations in the surface shell of ferrimagnetic nanoparticles plays a decisive role. According to this model, the magnetization enhancement is observed only in the case when the effect of the nonequilibrium cation distribution in the shell dominates over the effect of spin canting (*e.g.*, the case of $MgFe_2O_4$ and of $ZnFe_2O_4$).[57,58] Otherwise, a reduced magnetization (a phenomenon that is more frequently reported in the literature) may be expected for ferrite nanoparticles (*e.g.*, the case of $NiFe_2O_4$ and of $MnFe_2O_4$).[48,49] The case of the mechanosynthesized $BiFeO_3$ perovskite[28] clearly demonstrates that, in contrast to spinels, an enhanced magnetization in nanoferrite can also be caused by canted surface spins surrounding an antiferromagnetic core of nanoparticles.

The mechanosynthesis of Al-doped garnet-like $Li_7La_3Zr_2O_{12}$, which is one of the fastest chemically stable Li ion conductors known, represents an illustrative example for the benefits of high-energy ball milling. Cubic $Li_7La_3Zr_2O_{12}$, whose structure is stabilized against the tetragonal form by the incorporation of Al ions, can be prepared by co-milling of the binary oxides (Li_2O, ZrO_2, Al_2O_3, and La_2O_3) for 8 h in a Pulverisette 7 planetary mill.[59] Although a subsequent annealing step at elevated temperature is needed to obtain phase pure Al-doped cubic $Li_7La_3Zr_2O_{12}$, see Fig. 14, the necessary temperature of 873 K is much lower than that used in conventional solid state synthesis. Remarkably, it is even lower than the calcination temperature of a sol–gel synthesis route. In addition, compared to conventional solid state syntheses the mechanochemically assisted preparation of $Li_7La_3Zr_2O_{12}$ takes advantage of a very short sintering period of only 6 h. Most importantly, the low reaction temperature enabled the precise adjustment of the samples' stoichiometry since volatilization of Li could be largely prevented. This allowed a systematic investigation of the properties of Al-doped $Li_7La_3Zr_2O_{12}$. In particular, it turned out that the substitution of Al ions for La and Zr ions considerably affects the structure as well as the corresponding Li ion dynamics of garnet-type $Li_7La_3Zr_2O_{12}$.[59]

Nanostructured oxides prepared by mechanochemical methods are often inherently unstable owing to their far-from-equilibrium structural configurations. The last two examples presented are related to the *stability* of mechanosynthesized nanooxides at elevated temperatures and changing environments in which these nanostructures are expected to operate.

Fig. 15 shows the room-temperature ^{57}Fe Mössbauer spectra of mechanosynthesized $NiFe_2O_4$ spinel taken after annealing at various temperatures. Note that the near-surface layers of the mechanosynthesized spinel exhibit a nearly random cation distribution, deformed FeO_4 and FeO_6 polyhedra, and a canted spin arrangement.[48] The thermal stability range of such far-from-equilibrium configurations in the mechanosynthesized $NiFe_2O_4$ is found to extend up to 673 K. However, at $T > 673$ K, the superparamagnetic doublet, being characteristic of mechanosynthesized ferrite nanoparticles at room temperature, gradually vanishes because of particle growth of the spinel phase (Fig. 15). Simultaneously, the sextet structure, typical of the long-range ferrimagnetic state, develops because of the thermally induced changes in the spin configurations. The spectrum of the

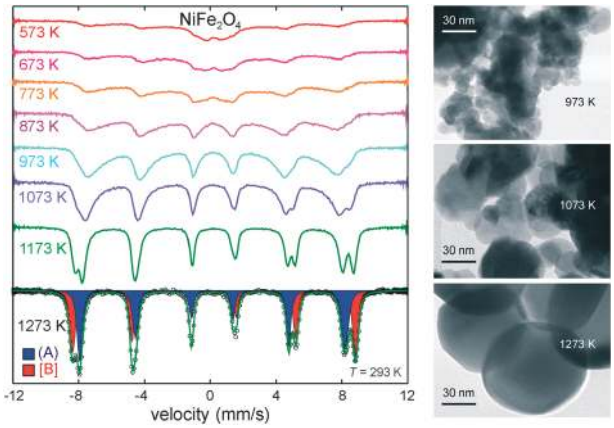

Fig. 15 (left) Room-temperature ^{57}Fe Mössbauer spectra of mechanosynthesized $NiFe_2O_4$ after annealing at various temperatures for 30 min. The annealing temperatures are shown in the figure. (right) TEM bright-field images of the material after annealing at 973, 1073, and 1273 K reveal different particle sizes. Reproduced with permission from ref. 48, copyright 2007 American Chemical Society.

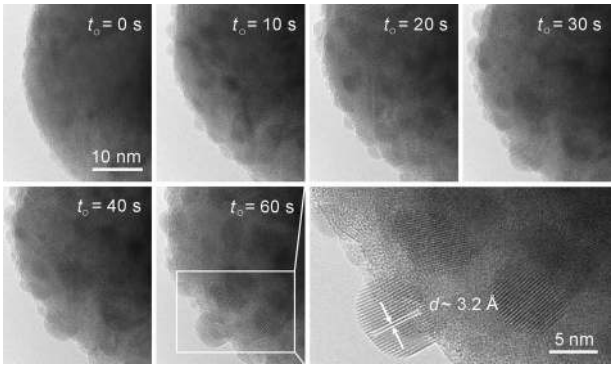

Fig. 17 *In situ* high-resolution TEM observation of the crystallization of the amorphous near-surface layers of mechanosynthesized $BiFeO_3$ perovskite. A metastability of the mechanically induced high-energy surface states manifests itself by the rapid crystallization reaction on the electron irradiation in the course of TEM investigations. The observation time (t_o) is shown in the figure. Reproduced with permission from ref. 28, copyright 2011 American Chemical Society.

mechanosynthesized $NiFe_2O_4$ after annealing at 1273 K (Fig. 15, bottom) consists of two sextets whose hyperfine magnetic field values are very similar to those found for a coarse-grained $NiFe_2O_4$. The quantitative evaluation of this spectrum revealed that the annealed sample exhibits the fully inverse spinel structure with a collinear spin alignment.[48] This case exemplarily gives evidence that mechanosynthesized materials are metastable, *i.e.*, at elevated temperatures they relax toward their equilibrium configuration.

The thermally induced relaxation processes in mechanosynthesized oxides are accompanied by changes in their functional properties. This is shown in Fig. 16 for magnetic spinels; their response to changes in temperature manifests itself by an alteration of the saturation magnetization. As can be seen, this quantity can be enhanced (for $NiFe_2O_4$)[48] or reduced (for $MgFe_2O_4$)[57] with increasing annealing temperature (*i.e.*, with increasing D). Obviously, this large variation in magnetization offers an ample opportunity to manipulate and tailor the magnetic properties of these nanomaterials.

It is found that the stability of mechanosynthesized nanoparticles is determined to a large extent by the nature of structural disorder of their near-surface/interface regions.

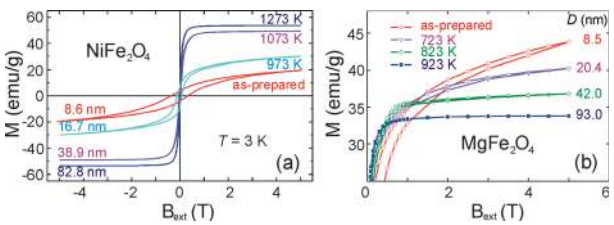

Fig. 16 Hysteresis loops measured at 3 K for mechanosynthesized and subsequently annealed (a) $NiFe_2O_4$ and (b) $MgFe_2O_4$. The annealing temperatures and the corresponding particle sizes are shown in the figure. Reproduced with permission from ref. 48 (a), copyright 2007 American Chemical Society. Reproduced with permission from ref. 57 (b), copyright 2007 Elsevier Science B.V.

In the case of amorphous surfaces/interfaces such as those detected in mechanosynthesized $BiFeO_3$,[28] the nanomaterial is found to respond even to a small change in environment in the course of TEM investigations. Fig. 17 documents the rapid kinetics of the electron beam-induced crystallization of the near-surface layers of mechanosynthesized $BiFeO_3$ perovskite observed under *in situ* conditions. This finding can be interpreted as a reaction of the mechanically induced high-energy surface states to electron irradiation. This observation demonstrates both the inherent instability and the high reactivity of "fresh" mechanosynthesized surfaces.

Based on the analogy with the electron beam-induced nucleation and growth processes presented above, we can state that the structurally disordered (amorphous) surfaces/interfaces play an essential role in the mechanically induced formation reactions; the impact-induced nucleation and growth processes of the mechanosynthesized phase are spatially confined to these highly deformed regions. It may be assumed that during the early stages of high-energy ball milling the reaction precursors are mixed at the atomic level and a new mechanosynthesized phase nucleates in interfacial regions between the solid reactants during the impact period. The growth mechanism of nuclei (crystallites) of the new phase could be understood as a result of the competitive effects of the impact-induced local heating and strains. The latter are accompanied by the amorphization (defect formation) of repeatedly impacted surfaces whereas the involved "thermal spikes" cause their crystallization. Note that similarly to the case of $BiFeO_3$,[28] the mechanism of mechanosynthesis of other perovskites (*e.g.*, $NaNbO_3$) has also been interpreted as being due to "nucleation-and-growth" processes from the amorphous phase.[60]

Concluding remarks

Mechanochemistry as a branch of chemistry, being concerned with the chemical and physical transformations of solids induced by mechanical action, has a long history and continues

to be of high importance. The chemical reactions of oxides induced by mechanical action can be categorized along the same lines that are commonly used in chemistry; they are either of homogeneous or of heterogeneous type. In the present review, the nature of the homogeneous mechanochemical reactions in oxides is highlighted by examples focusing on mechanically induced cation redistributions and canted spin arrangements, changes in the geometry of constitutive polyhedra, mechanically triggered formation of defective cation centers with unsaturated oxygen coordinations, and on mechanically induced phase transformations. Heterogeneous processes are illustrated by the mechanosyntheses of different families of complex oxides (stannates, silicates, ferrites, lanthanates) with a variety of structure types (spinel, orthorhombic, olivine, perovskite, garnet). These oxides can be mechanosynthesized at ambient temperature directly from their precursors in the form of nanosized powders, without the need for calcination at intermediate temperatures, thus making the process very simple. Due to the ability of spectroscopic methods (NMR, Mössbauer spectroscopy, XPS, Raman spectroscopy) and of high-resolution electron microscopy to provide structural information on a local atomic scale, valuable insight into the mechanochemically induced reactions in oxides is obtained. It is demonstrated that homogeneous and heterogeneous mechanochemical reactions of oxides are spatially confined to their interfacial regions with the thickness of about 1 nm. Functional properties and stability of oxides prepared by mechanochemical routes are determined to a large extent by a far-from-equilibrium structural state of their interface/near-surface regions.

The event of mechanically induced reactions provides novel opportunities for the non-thermal manipulation of materials and for the tailoring of their properties. The non-conventional mechanochemical approach offers several advantages over traditional processing routes including low-temperature solid state reactions, fewer processing steps, and suitability for the low cost, large-scale production of powders with nanosized crystallites. In this respect, mechanochemistry contributes to the search for novel sustainable production routes of functionally tailored nanomaterials. Although a surge of investigations in the field of mechanochemistry has resulted in the preparation of various metastable solids, the understanding of the fundamental mechanisms and kinetics of mechanochemical reactions has still not reached a satisfactory level, with the main reason probably being the complexity of these reactions and the shortage of systematic studies. A breakthrough in this context appears to be made in a very recent real-time study of mechanochemical transformations in a ball mill by means of *in situ* diffraction of high-energy synchrotron X-rays.[61]

In respect of modern technological challenges, a few examples[5] of the possible future application of mechanochemically prepared oxides should be mentioned: the high-energy ball milling process appears as a promising way to increase the performance of membrane materials for oxygen separation (*e.g.*, $Ba_{0.5}Sr_{0.5}Co_{0.5}Fe_{0.5}O_{3-\delta}$). Structural modification induced in ground oxide powders (*e.g.*, ZnO) has been reported to be useful for increasing their antibacterial effect. The mechanically activated iron-containing oxides are interesting for treatment of wastewaters, *e.g.*, milled Fe_3O_4 is very effective in the removal of arsenic from aqueous solutions, which allows one to keep the concentration of the residual arsenic below the regulation limits for drinking water. The electrochemical performance of oxide electrodes (*e.g.*, the $LiNi_{0.4}Co_{0.2}Mn_{0.4}O_2$ cathode and the Zn_2SnO_4 anode) has been found to be improved by the mechanochemical preparation route. Finally, mechanical activation has also been shown to be an important step in the preparation of photocatalytically active oxides (*e.g.*, N, S and Fe doped TiO_2 powders).[5]

Acknowledgements

The present work is supported by the DFG within the framework of the Priority Program ''*Crystalline Nonequilibrium Phases*'' (SPP 1415). Partial support from the APVV (project 0528-11), the VEGA (2/0174/11) and the Alexander von Humboldt Foundation is gratefully acknowledged. P.H. and M.W. acknowledge additional support by the DFG within the Research Unit 1277. K.-D.B. thanks the DFG and the State of Niedersachsen for support.

Notes and references

1 L. Takacs, *J. Mater. Sci.*, 2004, **39**, 4987 and references therein.
2 V. V. Boldyrev and K. Tkáčová, *J. Mater. Synth. Process.*, 2000, **8**, 121 and references therein.
3 S. Kipp, V. Šepelák and K. D. Becker, *Chem. Unserer Zeit*, 2005, **39**, 384 and references therein.
4 M. Carey Lea, *Am. J. Sci.*, 1892, **43**, 527, 3rd Series.
5 V. Šepelák, S. Bégin-Colin and G. Le Caër, *Dalton Trans.*, 2012, **41**, 11927 and references therein.
6 W. Ostwald, *Handbuch der Allgemeinen Chemie, Band 1*, Akademische Verlagsgesellschaft mbH, Leipzig, 1919, vol. 70.
7 G. Heinicke, *Tribochemistry*, Akademie Verlag, Berlin, 1984.
8 J. S. Benjamin, *Metall. Trans.*, 1970, **1**, 2943.
9 E. Avvakumov, M. Senna and N. Kosova, *Soft Mechanochemical Synthesis: A Basis for New Chemical Technologies*, Kluwer Academic Publishers, Boston, 2001.
10 C. Suryanarayana, *Prog. Mater. Sci.*, 2001, **46**, 1.
11 E. Gaffet and G. Le Caër, in *Encyclopedia of Nanoscience and Nanotechnology*, ed. H. S. Nalwa, American Scientific Publishers, Los Angeles, 2004, vol. 5, pp. 91–129.
12 M. K. Beyer and H. Clausen-Schaumann, *Chem. Rev.*, 2005, **105**, 2921.
13 V. Šepelák, I. Bergmann, S. Kipp and K. D. Becker, *Z. Anorg. Allg. Chem.*, 2005, **631**, 993.
14 V. V. Boldyrev, *Russ. Chem. Rev.*, 2006, **75**, 177.
15 B. Kubias, M. J. G. Fait and R. Schlögl, *Mechanochemical Methods*, in *Handbook of Heterogeneous Catalysis*, ed. G. Ertl, H. Knözinger, F. Schüth and J. Weitkamp, Wiley-VCH, Weinheim, 2008, vol. 1.
16 P. Baláž, *Mechanochemistry in Nanosciences and Minerals Engineering*, Springer-Verlag, Berlin, 2008.
17 F. Delogu and G. Mulas, *Experimental and Theoretical Studies in Modern Mechanochemistry*, Transworld Research Network, Kerala, 2010, and references therein.

18 P. Heitjans and S. Indris, *J. Mater. Sci.*, 2004, **39**, 5091.
19 *Mechanoresponsive Materials*, ed. C. Weder, *J. Mater. Chem.*, 2011, **21**, 8217–8476.
20 S. L. James, C. J. Adams, C. Bolm, D. Braga, P. Collier, T. Friščić, F. Grepioni, K. D. M. Harris, G. Hyett, W. Jones, A. Krebs, J. Mack, L. Maini, A. G. Orpen, I. P. Parkin, W. C. Shearouse, J. W. Steed and D. C. Waddell, *Chem. Soc. Rev.*, 2012, **41**, 413 and references therein.
21 D. Krüger, R. Rousseau, H. Fuchs and D. Marx, *Angew. Chem., Int. Ed.*, 2003, **42**, 2251.
22 Website of the Institute of Solid State Chemistry and Mechanochemistry, Novosibirsk; http://www.solid.nsc.ru/.
23 K. Tkáčová, *J. Mater. Synth. Process.*, 2000, **8**, 119.
24 *Mechanochemistry and Mechanical Alloying 2003*, ed. V. Šepelák, K. D. Becker and Z. A. Munir, *J. Mater. Sci.*, 2004, **39**, 4983–5530.
25 IUPAC. *Compendium of Chemical Terminology*, 2nd edn (the "Gold Book"). Compiled by A. D. McNaught and A. Wilkinson. Blackwell Scientific Publications, Oxford (1997). XML on-line corrected version: http://goldbook.iupac.org (2006) created by M. Nic, J. Jirat and B. Kosata; updates compiled by A. Jenkins. ISBN 0-9678550-9-8.
26 V. Šepelák, M. Myndyk, M. Fabián, K. L. Da Silva, A. Feldhoff, D. Menzel, M. Ghafari, H. Hahn, P. Heitjans and K. D. Becker, *Chem. Commun.*, 2012, **48**, 11121.
27 A. Mann, *Nature*, 2011, **475**, 280.
28 K. L. Da Silva, D. Menzel, A. Feldhoff, C. Kübel, M. Bruns, A. Paesano, Jr., A. Düvel, M. Wilkening, M. Ghafari, H. Hahn, F. J. Litterst, P. Heitjans, K. D. Becker and V. Šepelák, *J. Phys. Chem. C*, 2011, **115**, 7209 and references therein.
29 V. Šepelák and K. D. Becker, *J. Mater. Synth. Process.*, 2000, **8**, 155.
30 K. Tkáčová, *Mechanical Activation of Minerals*, Elsevier, Amsterdam, 1989.
31 P. Heitjans and S. Indris, *J. Phys.: Condens. Matter*, 2003, **15**, R1257 and references therein.
32 P. Heitjans and M. Wilkening, *Diffus. Defect Data, Pt. A*, 2009, **283–286**, 705 and references therein.
33 M. Wilkening, V. Epp, A. Feldhoff and P. Heitjans, *J. Phys. Chem. C*, 2008, **112**, 9291.
34 V. Šepelák, I. Bergmann, S. Indris, A. Feldhoff, H. Hahn, K. D. Becker, C. P. Grey and P. Heitjans, *J. Mater. Chem.*, 2011, **21**, 8332.
35 V. Šepelák and K. D. Becker, *J. Korean Ceram. Soc.*, 2012, **49**, 19.
36 V. Šepelák, K. Tkáčová, V. V. Boldyrev, S. Wißmann and K. D. Becker, *Physica B*, 1997, **234–236**, 617.
37 V. Šepelák, D. Baabe, F. J. Litterst and K. D. Becker, *J. App. Phys.*, 2000, **88**, 5884.
38 V. Šepelák, D. Baabe and K. D. Becker, *J. Mater. Synth. Process.*, 2000, **8**, 333.
39 V. Šepelák, S. Indris, I. Bergmann, A. Feldhoff, K. D. Becker and P. Heitjans, *Solid State Ionics*, 2006, **177**, 2487.
40 P. Druska, U. Steinike and V. Šepelák, *J. Solid State Chem.*, 1999, **146**, 13.
41 S. A. Oliver, V. G. Harris, H. H. Hamdeh and J. C. Ho, *Appl. Phys. Lett.*, 2000, **76**, 2761.
42 V. Šepelák, D. Baabe, D. Mienert, D. Schultze, F. Krumeich, F. J. Litterst and K. D. Becker, *J. Magn. Magn. Mater.*, 2003, **257**, 377.
43 S. A. T. Redfern, R. J. Harrison, H. S. C. O'Neill and D. R. R. Wood, *Am. Mineral.*, 1999, **84**, 299.
44 Z. Wang, P. Lazor, S. K. Saxena and G. Artioli, *J. Solid State Chem.*, 2002, **165**, 165.
45 K. E. Sickafus, A. C. Larson, N. Y. M. Nastasi, G. W. Hollenberg, F. A. Garner and R. C. Bradt, *J. Nucl. Mater.*, 1995, **219**, 128.
46 V. Šepelák, M. Menzel, K. D. Becker and F. Krumeich, *J. Phys. Chem. B*, 2002, **106**, 6672.
47 V. Šepelák, A. Feldhoff, P. Heitjans, F. Krumeich, D. Menzel, F. J. Litterst, I. Bergmann and K. D. Becker, *Chem. Mater.*, 2006, **18**, 3057.
48 V. Šepelák, I. Bergmann, A. Feldhoff, P. Heitjans, F. Krumeich, D. Menzel, F. J. Litterst, S. J. Campbell and K. D. Becker, *J. Phys. Chem. C*, 2007, **111**, 5026.
49 M. Muroi, R. Street, P. G. McCormick and J. Amighian, *Phys. Rev. B: Condens. Matter Mater. Phys.*, 2001, **63**, 184414.
50 V. Šepelák, S. M. Becker, I. Bergmann, S. Indris, M. Scheuermann, A. Feldhoff, C. Kübel, M. Bruns, N. Stürzl, A. S. Ulrich, M. Ghafari, H. Hahn, C. P. Grey, K. D. Becker and P. Heitjans, *J. Mater. Chem.*, 2012, **22**, 3117.
51 L. J. Berchmans, M. Myndyk, K. L. Da Silva, A. Feldhoff, J. Šubrt, P. Heitjans, K. D. Becker and V. Šepelák, *J. Alloys Compd.*, 2010, **500**, 68.
52 V. Šepelák, K. D. Becker, I. Bergmann, S. Suzuki, S. Indris, A. Feldhoff, P. Heitjans and C. P. Grey, *Chem. Mater.*, 2009, **21**, 2518 and references therein.
53 P. Heitjans and M. Wilkening, *MRS Bull.*, 2009, **34**, 915.
54 A. Düvel, E. Romanova, M. Sharifi, D. Freude, M. Wark, P. Heitjans and M. Wilkening, *J. Phys. Chem. C*, 2011, **115**, 22770 and references therein.
55 J. H. Kwak, J. Hu, D. Mei, C.-W. Yi, D. H. Kim, C. H. F. Peden, L. F. Allard and J. Szanyi, *Science*, 2009, **325**, 1670.
56 V. Šepelák, U. Steinike, D. C. Uecker, S. Wißmann and K. D. Becker, *J. Solid State Chem.*, 1998, **135**, 52.
57 V. Šepelák, I. Bergmann, D. Menzel, A. Feldhoff, P. Heitjans, F. J. Litterst and K. D. Becker, *J. Magn. Magn. Mater.*, 2007, **316**, e764.
58 V. Šepelák, D. Baabe, D. Mienert, F. J. Litterst and K. D. Becker, *Scr. Mater.*, 2003, **48**, 961.
59 A. Düvel, A. Kuhn, L. Robben, M. Wilkening and P. Heitjans, *J. Phys. Chem. C*, 2012, **116**, 15192 and references therein.
60 T. Rojac, B. Malič, M. Kosec, M. Połomska, B. Hilczer, B. Zupančič and B. Zalar, *Solid State Ionics*, 2012, **215**, 1 and references therein.
61 T. Friščić, I. Halasz, P. J. Beldon, A. M. Belenguer, F. Adams, S. A. J. Kimber, V. Honkimäki and R. E. Dinnebier, *Nature Chem.*, 2013, **5**, 66.

